Anisotropic Three-Dimensional Magnetism in $CaFe_2As_2$

R. J. McQueeney,[1,2] S. O. Diallo,[2] V. P. Antropov,[2] G. D. Samolyuk,[2] C. Broholm,[3] N. Ni,[1,2] S. Nandi,[1,2] M. Yethiraj,[4] J. L. Zarestky,[2] J. J. Pulikkotil,[2] A. Kreyssig,[1,2] M. D. Lumsden,[5] B. N. Harmon,[1,2] P. C. Canfield,[1,2] and A. I. Goldman[1,2]

[1]*Department of Physics & Astronomy, Iowa State University, Ames, Iowa 50011, USA*
[2]*Ames Laboratory, Ames, Iowa 50011, USA*
[3]*Department of Physics & Astronomy, Johns Hopkins University, Baltimore, Maryland 21218 USA*
[4]*Bragg Institute, ANSTO, PMB 1, Menai NSW 2234, Australia*
[5]*Oak Ridge National Laboratory, Oak Ridge, Tennessee 37831, USA*

(Received 10 September 2008; published 26 November 2008)

Inelastic neutron scattering measurements of the magnetic excitations in $CaFe_2As_2$ indicate that the spin wave velocity in the Fe layers is exceptionally large and similar in magnitude to the cuprates. However, the spin wave velocity perpendicular to the layers is at least half as large that in the layer, so that the magnetism is more appropriately categorized as anisotropic three-dimensional, in contrast to the two-dimensional cuprates. Exchange constants derived from band structure calculations predict spin wave velocities that are consistent with the experimental data.

DOI: 10.1103/PhysRevLett.101.227205 PACS numbers: 75.30.Ds, 74.72.−h, 75.30.Et, 78.70.Nx

The observations of antiferromagnetic (AFM) ordering [1] in the new class of iron-based superconductors (SC), its subsequent suppression upon chemical doping or changes in stoichiometry [2,3], and the eventual appearance of SC [4,5] are reminiscent of the high-temperature superconducting cuprates [6]. Such similarities might suggest a common origin for SC and indeed AFM spin fluctuations have been proposed as a possible pairing mechanism in both the cuprates [7] and the iron arsenides [8]. Thus, it is important to compare the details of the magnetic interactions in these two systems. In the cuprates, strong superexchange interactions are present in the AFM insulating (parent) phase and give rise to a high AFM ordering temperature ($T_N \sim 300$ K) [9]. Furthermore, the magnetic interactions in the cuprates have a strong two-dimensional (2D) anisotropy due to the weak coupling between the CuO_2 layers [10]. The iron arsenide superconductors also have layered structures and high Néel temperatures (100–200 K). However, the parent phases of the iron arsenides are not insulators. Rather, they are metallic and, for the AFe_2As_2 (A = Ca, Sr, Ba) compounds, the AFM ordering is strongly coupled to a structural transition from a high-temperature tetragonal structure to a low temperature orthorhombic structure [11]. One other notable difference between the cuprates and iron arsenides concerns the conditions necessary for SC. While doping charge carriers does indeed suppress AFM and the structural transition and lead to SC in both systems, it has recently been shown that pressure alone can destroy the AFM state in $CaFe_2As_2$ and lead to SC [12,13]. The appearance of SC in $CaFe_2As_2$ upon the suppression of both a structural phase transformation and AFM ordering leaves open the possibility for either phonon mediated or spin fluctuation mediated superconductivity.

In this Letter, we explore the magnetic interactions in the parent $CaFe_2As_2$ compound. Despite the differences between the cuprates and arsenides noted above, the energy scale and dimensionality (or anisotropy) of the magnetic interactions may actually be quite similar, possibly leading to a common origin for SC in these two families of compounds. To move beyond qualitative comparisons and explore the potential relevance of magnetic interactions to SC in the iron arsenides, direct measurements of the energy scale and anisotropy of the magnetic interactions are necessary. The strength and anisotropy of the magnetic interactions in the parent compound forms the basis for the evolution of spin correlations under superconducting conditions. Here we report on inelastic neutron scattering measurements from $CaFe_2As_2$ and demonstrate that the magnetic exchange interactions in the Fe layers are exceptionally large, with an energy scale similar in magnitude to the cuprates. Although the magnetic exchange between the Fe layers is relatively small ($>\sim$10% of the in-plane exchange), it is substantially larger than that found for the cuprates ($\sim$0.001%). This anisotropic three-dimensional (3D) magnetism is consistent with *ab initio* calculations of the spin dynamics.

$CaFe_2As_2$ is a metallic parent compound that becomes superconducting upon either doping [14] or application of pressure [13]. In this respect, $CaFe_2As_2$ is a model compound for studying the development of superconductivity. $CaFe_2As_2$ orders in a columnar-type AFM structure [as shown in Fig. 1(a)] coincident with a structural transition from a tetragonal ($I4/mmm$) to an orthorhombic ($Fmmm$) crystal structure below $T_s = 172$ K and having lattice parameters $a = 5.51$ Å, $b = 5.45$ Å, and $c = 11.66$ Å at $T = 10$ K [11]. For the inelastic neutron scattering study, single crystals of $CaFe_2As_2$ were grown out of Sn flux using conventional high-temperature solution growth techniques described previously [15]. Crystals were etched in concentrated hydrochloric acid to remove Sn flux from the surface. Measurements were performed on a $\sim$1 gram

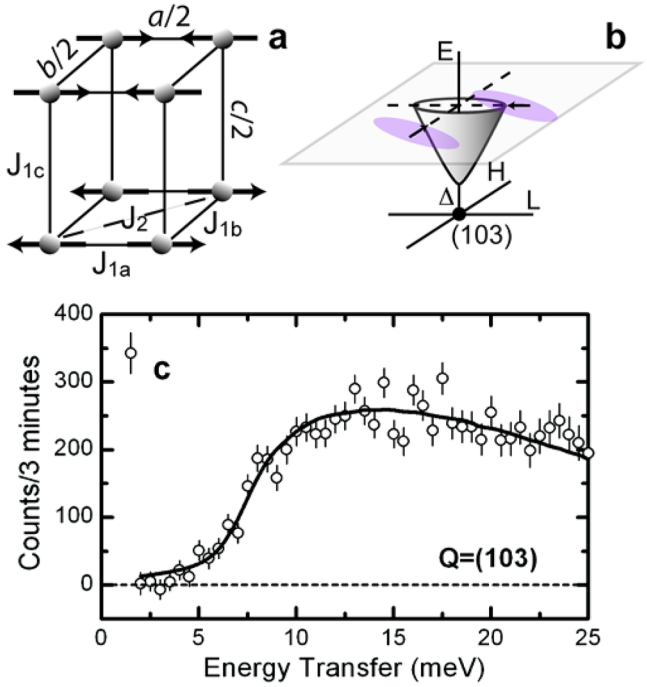

FIG. 1 (color online). (a) The magnetic structure (showing Fe atoms only) and exchange interactions in $CaFe_2As_2$ [11]. (b) Schematic picture of an antiferromagnetic conical spin wave dispersion surface that is consistent with the data. The shaded plane indicates a constant-energy surface, and the shaded ellipses represent the orientation of the resolution ellipsoid for H and L scans. (c) Intensity as a function of neutron energy loss at $T = 14$ K at the magnetic zone center, $\mathbf{Q}_{\mathbf{AFM}} = (1, 0, 3)$. The solid black line shows fits to the data using the model dispersion [Eq. (1)] convoluted with the instrumental resolution function.

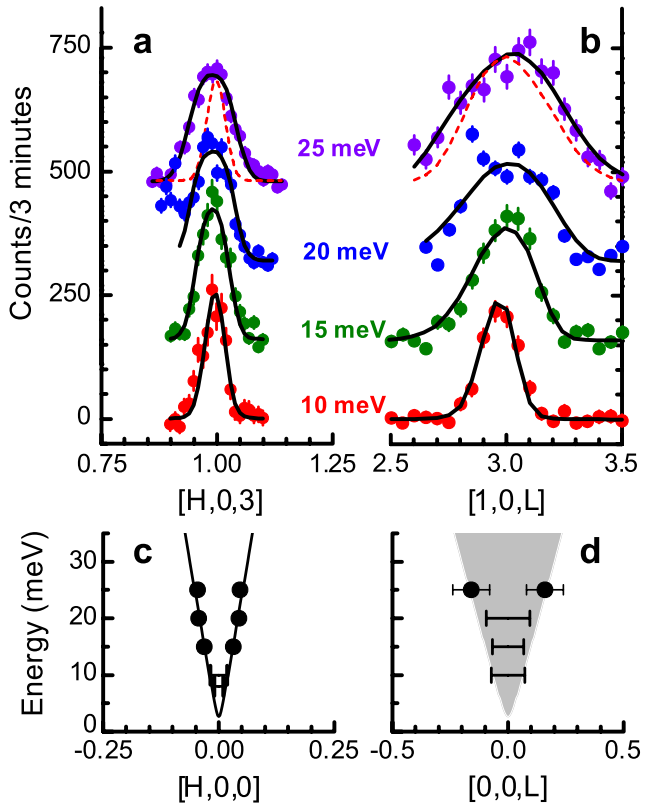

FIG. 2 (color online). (a) Intensity along the H direction near $\mathbf{Q}_{\mathbf{AFM}} = (1, 0, 3)$ at several different energies. Scans at different energies are vertically offset by 160 counts. (b) Constant-energy scans along L. In (a) and (b), the solid black lines are fits to the data using the model dispersion [Eq. (1)] convoluted with the instrumental resolution function. Dashed lines are estimates of the line shape at 25 meV that would result from an infinitely steep dispersion surface. (c) The plotted model dispersion along the (H00) direction (black line). (d) The model dispersion along the (00L) direction is plotted as a shaded region, indicating that the data only provide a lower bound on the spin wave velocity along L. In (c) and (d), fitted data points are indicated by black circles and lower bounds to the dispersion are indicated by vertical lines connected by a bar.

coaligned single-crystal composite mounted in the [$H0L$] scattering plane (in orthorhombic notation) with a measured mosaic of 1.5° (full-width-at-half-maximum) for both (H00) and (00L) reflections. The sample was mounted on the cold finger of a closed-cycle helium refrigerator. Measurements were performed on the HB-3 triple-axis spectrometer at the High Flux Isotope Reactor at Oak Ridge National Laboratory. Pyrolitic graphite monochromator and analyzer crystals were used with a fixed final neutron energy $E_f = 14.7$ meV and horizontal collimations of $48' - 40' - 80' - 120'$.

Figures 1 and 2 show evidence for collective magnetic excitations at temperatures well below T_s ($T = 14$ K). Figure 1(b) shows a schematic drawing of a dispersion surface in the [$H0L$] plane near the magnetic Bragg peak that is consistent with our observations. As discussed below, the energy of the observed excitations is well below the maximum (Brillouin zone boundary) spin wave energy. Therefore, the scattering data can be interpreted as resulting from coherent spin waves in the small-$\mathbf{q}$ approximation with an anisotropic conical dispersion in the [$H0L$] plane and a small energy gap, Δ, as illustrated in Fig. 1(b). The spectral gap at the magnetic Bragg peak ($\mathbf{Q}_{\mathbf{AFM}}$) is clearly demonstrated in Fig. 1(c), which displays an energy scan at $\mathbf{Q}_{\mathbf{AFM}} = (1, 0, 3)$. The background was removed by subtracting a similar spectrum acquired at (1.15,0,3). The data indicate an onset of magnetic scattering above approximately 5–6 meV. Further, Fig. 1(c) shows significant spectral weight up to 25 meV (the kinematic limit of the present experiment) with little intensity loss, implying that the magnetic energy scale actually extends to much higher energies.

In order to map the dispersion in the vicinity of $\mathbf{Q}_{\mathbf{AFM}}$, constant-energy scans along the [H00] and [00L] directions were performed near the $\mathbf{Q}_{\mathbf{AFM}} = (1, 0, 3)$ and are shown in Figs. 2(a) and 2(b). If there are in fact propagating spin waves in $CaFe_2As_2$, the constant-energy scans should eventually reveal a peak splitting as the energy is increased. However, in $CaFe_2As_2$, the energy scale is large

enough (with a correspondingly steep dispersion) that the present measurements produce a single peak up to 25 meV due to the finite instrumental resolution [see Fig. 1(b)]. The measurement therefore cannot distinguish whether one is dealing with a single ridge of scattering or a sharp conical dispersion surface as expected for propagating spin waves. Nevertheless, the constant-energy cuts do broaden beyond the spectrometer resolution and the corresponding spin wave velocity (the slope of the dispersion in the linear range) can be obtained by fitting the data to a model function convoluted with the resolution function of the instrument. The data was modeled with an anisotropic conical dispersion with an energy gap (Δ) and different spin wave velocities in the Fe layers (*ab* plane) along $H(v_\parallel)$ [16] and perpendicular to the layers along L ($v_\perp$).

$$\varepsilon(\mathbf{q}) = \sqrt{\Delta^2 + v_\parallel^2(q_x^2 + q_y^2) + v_\perp^2 q_z^2} \tag{1}$$

Perhaps of greatest importance here is the anisotropy of the velocity ($v_\perp/v_\parallel$), which is a measure of the anisotropy of the magnetic interactions, with $v_\perp/v_\parallel = 1$ representing an isotropic 3D AFM and $v_\perp/v_\parallel \approx 0$ a 2D AFM. Neutron intensities were represented by a simple Lorentzian response with energy width Γ and oscillator strength varying as ω^{-1}.

$$S(\mathbf{Q}, \omega) = \frac{1}{\hbar\omega} \frac{A\hbar\Gamma/\pi}{(\hbar\omega - \varepsilon(\mathbf{Q} - \mathbf{Q_{AFM}}))^2 + (\hbar\Gamma)^2} \tag{2}$$

Here $\hbar\mathbf{Q}$ is momentum transfer, $\hbar\omega$ is energy transfer, and A is an overall scale factor. The model $S(\mathbf{Q}, \omega)$ was convoluted with the resolution function of the spectrometer and fit to the data using the RESLIB program [17] and the instrument parameters listed above. A small damping factor, $\hbar\Gamma$ was fixed at 1 meV (below the resolution limit) to facilitate the numerical convolutions.

The energy gap, $\Delta = 6.9 \pm 0.2$ meV, was determined from a fit to the $T = 14$ K energy scan in Fig. 1(c). The in-plane spin wave velocity was obtained by fitting the constant-energy scans along the [H00] direction [Fig. 2(a)]. The highest energy cuts at 15, 20, and 25 meV, yield an average in-plane velocity of $v_\parallel = 420 \pm 70$ meV Å. The data at 10 meV yield only a lower bound of $v_\parallel > 300$ meV Å. Scans along the [00L] direction [Fig. 2(b)] are sensitive to the out-of-plane velocity. The [00L] constant-energy scans around (103) were, however, obtained in a defocused resolution condition, so that only the 25 meV scan provided a refinable value of $v_\perp = 270 \pm 100$ meV Å. The [00L] scans below 25 meV produce a lower bound, $v_\perp > 200$ meV Å below which the convoluted model functions are noticeably broader than the data. This minimum velocity condition is consistent with the value obtained at 25 meV. The corresponding dispersion curves are shown in Figs. 2(c) and 2(d). The scale factor (A) refined to a constant value within 15% for all fits, indicating that the expected ω^{-1} dependence of the cross-section is consistent with the data. As described above, the ratio of $v_\perp/v_\parallel > 0.5$ indicates the 3D nature of magnetism in $CaFe_2As_2$, in contrast to the quasi-2D cuprates (where $v_\perp/v_\parallel \approx 0$).

We now turn to theoretical calculations of the spin dynamics in $CaFe_2As_2$. Several papers address the nature of the magnetic interactions in the iron arsenic superconductors [18–22]. The magnetism is often discussed in a localized 2D Heisenberg model with short-ranged interactions where the interlayer exchange is assumed to be negligible (the $J_1 - J_2$ model). Because of our observation of 3D magnetic interactions, and the possible presence of itinerant magnetism in metallic $CaFe_2As_2$, the exchange interactions were calculated using Green's function formalism within the Atomic Sphere Approximation [23,24]. This theoretical technique has been recently applied to the related Fe-Se based superconductors [25]. Using the experimental orthorhombic structural parameters for $CaFe_2As_2$ [11], these calculations predict the observed columnar AFM structure with a moment size of $gS = 1.33\mu_B$ with $g \approx 2$ (somewhat larger than the observed moment of $0.8\mu_B$). The calculated pairwise magnetic exchange interactions are long-ranged, with dominant nearest-neighbor (NN) and next-nearest-neighbor (NNN) interactions. "Frozen" magnon calculations [23,24,26] of the spin wave velocities ($v_\parallel = 390$ meV Å, $v_\perp = 190$ meV Å) are in good agreement with those extracted from the present data.

Despite the presence of long-range interactions and itinerancy, it is useful to consider the simplest model that captures the essential physics in the magnetism of $CaFe_2As_2$. In the limit of small-q as measured here, even the most strongly itinerant systems can be parametrized by a Heisenberg model. We further simplify the Heisenberg model by retaining only NN and NNN interactions. The calculated NN exchange interactions are all AFM, with a strong orthorhombic anisotropy [27]; $SJ_{1a} = 41$ meV, $SJ_{1b} = 10$ meV, and $SJ_{1c} = 3$ meV [see Fig. 1(a)]. Appreciable NNN exchange ($SJ_2 = 21$ meV) is sufficiently large to stabilize the columnar AFM structure given that $\frac{1}{2}(J_{1a} + J_{1b})/J_2 = 1.2$ (fulfilling the condition that $J_1/J_2 < 2$ for the tetragonal structure [21,22]). The rather significant exchange along the c axis confirms the 3D nature of the system and indicates that $J_c/J_{1a} \sim 10\%$ for $CaFe_2As_2$, which is orders of magnitude larger than the cuprates, where $J_c/J_{1a} \sim 10^{-5}$. From the NNN Heisenberg exchanges, the calculated velocities are $v_\parallel = aS(J_{1a} + 2J_2)\sqrt{1 + J_{1c}/(J_{1a} + 2J_2)} = 450$ meV and $v_\perp = cSJ_{1c}\sqrt{1 + (J_{1a} + 2J_2)/J_{1c}} = 190$ meV Å and the calculated velocity ratio is

$$\frac{v_\perp}{v_\parallel} = \frac{c}{a}\sqrt{\frac{J_{1c}}{J_{1a} + 2J_2}} \approx 0.4. \tag{3}$$

Velocities within the NNN Heisenberg model are in surprisingly close agreement with the more general frozen

magnon calculations, implying that contributions of more distant interactions to the spin wave velocity largely cancel each other. Nonetheless, all of the calculated quantities are in good agreement with the data, suggesting that a fully anisotropic 3D NNN Heisenberg model can be applied to $CaFe_2As_2$ in the small-q limit. Neutron measurements on $SrFe_2As_2$ also report significant interlayer magnetic interactions [28]. However, the interlayer coupling in $CaFe_2As_2$ is several times larger than calculated in the closely related Fe-Se based superconductors [25], indicating that the degree of the anisotropy may vary substantially for the different iron-based superconductors.

The calculations also predict several details about the magnetic Hamiltonian that are beyond the reach of the present experiments. Using the numerical ''torque'' technique [26], the Green's function formalism yields a 2.1 meV spin gap due to spin-orbit coupling. This is significantly smaller than the measured gap ($\sim$7 meV) and indicates the presence of additional spin space anisotropies. The theoretical calculations estimate the ''itinerancy'' of the magnetic interactions as the ratio of the characteristic spin wave energy to the spin (Stoner) splitting of the electronic energy bands [29]. This ratio (0.2) places $CaFe_2As_2$ in the regime of a marginally itinerant magnet (similar to face-centered-cubic Fe) at the borderline between itinerant and localized behavior. As discussed above, the effect of itinerancy of $CaFe_2As_2$ is not apparent at small-q, but should appear at large-q near the Brillouin zone boundary in the form of spin wave decay into the electron-hole pair continuum. In addition, the calculations of the magnetic susceptibility predict that itinerancy gives rise to substantial longitudinal magnetic fluctuations similar to those discussed for the Fe-Se system [25].

In conclusion, despite the similarity of the magnetic energy scale in $CaFe_2As_2$ and the cuprates, there are substantial differences in the magnetic Hamiltonians. In the insulating cuprate parent compounds, the 2D Heisenberg model is dominant, and only lifted by small XY anisotropy and antisymmetric exchange interactions [30]. In $CaFe_2As_2$, there is substantial interlayer coupling and the presence of a spin gap indicates additional spin space anisotropies. Strictly 2D magnetic systems are characterized by large quantum spin fluctuations, which might mediate superconductivity. Our measurements provide evidence for strong 3D magnetic interactions in $CaFe_2As_2$ which should suppress quantum fluctuations when an ordered state satisfying all interactions exists. However, the large exchange interactions combined with magnetic frustration may be sufficient to support spin fluctuations in superconducting compositions.

The authors acknowledge useful discussions with J. Schmalian, D. Johnston, D. Argyriou, Z. Tesanovic, and A. Christianson. Work is supported by the U. S. Department of Energy Office of Science under the following contracts: at the Ames Laboratory under Contract No. DE-AC02-07CH11358 and at the Institute for Quantum Matter at Johns Hopkins University under Contract No. DE-FG02-08ER46544. Oak Ridge National Laboratory is supported by the Scientific User Facilities Division and by the Division of Materials Sciences and Engineering, Office of Basic Energy Sciences.

[1] C. de la Cruz *et al.*, Nature (London) **453**, 899 (2008).
[2] J. Zhao *et al.*, Nature Mater. [to be published (2008)].
[3] H. Chen *et al.*, arXiv:0807.3950.
[4] W. Lu *et al.*, Solid State Commun. **148**, 168 (2008).
[5] M. Rotter *et al.*, Angew. Chem., Int. Ed. **47**, 7949 (2008).
[6] T. Honma and P. H. Hor, Phys. Rev. B **77**, 184520 (2008).
[7] A. Chubukov, D. Pines, and J. Schmalian, in *The Physics of Conventional and Unconventional Superconductors*, edited by K. H. Bennemann and J. B. Ketterson (Springer-Verlag, Berlin, 2002), p. 495.
[8] I. I. Mazin and M. D. Johannes, arXiv:0807.3737.
[9] D. Vaknin *et al.*, Phys. Rev. Lett. **58**, 2802 (1987).
[10] Y. Endoh *et al.*, Phys. Rev. B **37**, 7443 (1988).
[11] A. I. Goldman *et al.*, Phys. Rev. B **78**, 100506 (2008).
[12] A. Kreyssig *et al.*, arXiv:0807.3032.
[13] M. S. Torikachvili *et al.*, Phys. Rev. Lett. **101**, 057006 (2008).
[14] G. Wu *et al.*, J. Phys. Condens. Matter **20**, 422201 (2008).
[15] N. Ni *et al.*, Phys. Rev. B **78**, 014523 (2008).
[16] It is assumed that spin wave velocities along H and K are the same, although theoretical calculations discussed below show that this is not true for the orthorhombic structure. In any case, the spin waves along K are not directly measured.
[17] A. Zheludev, RESLIB program.
[18] V. Cvetkovic and Z. Tesanovic, arXiv:0804.4678.
[19] C. Fang *et al.*, Phys. Rev. B **77**, 224509 (2008).
[20] M. M. Korshunov and I. Eremin, Europhys. Lett. **83**, 67 003 (2008).
[21] T. Yildirim, Phys. Rev. Lett. **101**, 057010 (2008).
[22] Q. Si and E. Abrahams, Phys. Rev. Lett. **101**, 076401 (2008).
[23] V. P. Antropov *et al.*, J. Appl. Phys. **99**, 08F507 (2006).
[24] M. van Schilfgaarde and V. P. Antropov, J. Appl. Phys. **85**, 4827 (1999).
[25] J. J. Pulikkotil, M. v. Schilfgaarde, and V. P. Antropov, arXiv:0809.0283.
[26] V. P. Antropov, B. N. Harmon, and A. N. Smirnov, J. Magn. Magn. Mater. **200**, 148 (1999).
[27] Calculations of the moment size and the magnitude of J_{1b} (or the in-plane exchange anisotropy) were found to be extremely sensitive to the position of As within the unit cell.
[28] J. Zhao *et al.*, Phys. Rev. Lett. **101**, 167203 (2008).
[29] V. P. Antropov, J. Magn. Magn. Mater. **262**, L192 (2003).
[30] M. A. Kastner *et al.*, Rev. Mod. Phys. **70**, 897 (1998).